Open Forum Infectious Diseases

MAJOR ARTICLE

Enterovirus D68: Genomic and Clinical Comparison of 2 Seasons of Increased Viral Circulation and Discrepant Incidence of Acute Flaccid Myelitis—Maryland, USA

Amary Fall,[1] Omar Abdullah,[1] Lijie Han,[1] Julie M. Norton,[1] Nicholas Gallagher,[1] Michael Forman,[1] C. Paul Morris,[2] Eili Klein,[3,4] and Heba H. Mostafa[1]

[1]Division of Medical Microbiology, Department of Pathology, Johns Hopkins School of Medicine, Baltimore, Maryland, USA, [2]Integrated Research Facility, Division of Clinical Research, National Institute of Allergy and Infectious Diseases, National Institutes of Health, Frederick, Maryland, USA, [3]Department of Emergency Medicine, Johns Hopkins School of Medicine, Baltimore, Maryland, USA, and [4]Center for Disease Dynamics, Economics, and Policy, Washington DC, USA

Background. Enterovirus D68 (EV-D68) is associated with severe respiratory disease and acute flaccid myelitis (AFM). The 2022 outbreaks showed increased viral circulation and hospital admissions, but the expected rise in AFM cases did not occur. We analyzed EV-D68 genomes and infection outcomes from 2022 (a year without a national increase in AFM cases) and 2018 (a year with a national surge in AFM cases) to understand how viral genomic changes might influence disease outcomes.

Methods. Residual respiratory samples that tested positive for rhinovirus/enterovirus at the Johns Hopkins Health System between 2018 and 2022 were collected for EV-D68 polymerase chain reaction, genotyping, and whole genome sequencing. Clinical and metadata were collected in bulk from the electronic medical records.

Results. A total of 351 EV-D68 cases were identified, with most cases in children aged <5 years. Infections in 2018 were associated with higher odds of hospital admissions and intensive care unit care. Of 272 EV-D68 genomes, subclades B3 and A2/D1 were identified with B3 predominance (95.2%). A comparative analysis of the 2018 and 2022 whole genomes identified a cluster of amino acids (554D, 650T, 918T, 945N, 1445I, 1943I) that was associated with higher odds of severe outcomes.

Conclusions. Our results show significant differences in the clinical outcomes of EV-D68 infections in 2018 and 2022 and highlight a 2018 cluster of genomic changes associated with these differences. Seasonal viral genomic surveillance—with in vitro characterization of the significance of these changes to viral fitness, immune responses, and neuropathogenesis—should shed light on the viral determinants of AFM.

Keywords. acute flaccid myelitis; AFM; enterovirus D68; EV-D68; paralysis.

Enterovirus D68 (EV-D68), first characterized in 1962, was infrequently reported for several decades. However, since 2014, EV-D68 outbreaks with increased circulation and respiratory disease have recurred every 2 years (2014, 2016, and 2018) in the United States and many other countries. Notably, these outbreaks were associated with increased cases of acute flaccid myelitis (AFM), a serious paralytic condition primarily affecting children [1].

The biennial pattern of EV-D68 circulation was interrupted by the COVID-19 pandemic, resulting in low case numbers worldwide in 2020 and 2021 [2–6]. In 2022, outbreaks of EV-D68 led to increased pediatric hospital admissions for severe respiratory illness in the United States and Europe [7–9]. Interestingly, the 2022 resurgence of EV-D68 was not associated with a rise in AFM cases, which remained low and were clinically different from cases reported in 2018, a peak AFM year [1]. This suggests a change in disease outcomes and the association between EV-D68 infection and AFM.

Understanding the viral genomic determinants of outbreaks and neuropathogenicity could improve our knowledge of AFM and the determinants of severity of respiratory disease, enhance epidemiologic surveillance, and aid in identifying therapeutic and vaccine targets.

Notably, viral causes of neurologic disease may be undetectable in patients who present later in the disease course [10]. Additionally, viruses are rarely detected in the cerebrospinal fluid (CSF) of patients with AFM [11, 12]. Therefore, understanding the patterns of community respiratory transmission, viral genomic evolution, and local or national AFM trends is crucial for evaluating the association between EV-D68 and neurologic disease. In this study, we compared 2 cohorts of patients with EV-D68 and viral genomes from 2 seasons

Received 16 September 2024; editorial decision 31 October 2024; accepted 01 November 2024; published online 19 November 2024

Correspondence: Heba H. Mostafa, MD, PhD, D(ABMM), Meyer B-121F, 600 N. Wolfe St, Baltimore, MD 21287 (hmostaf2@jhmi.edu); Eili Klein, PhD, 5801 Smith Ave, Davis Suite 3220, Baltimore, MD 21209 (eklein@jhu.edu).

Open Forum Infectious Diseases®

https://doi.org/10.1093/ofid/ofae656

with increased EV-D68 circulation but differing national AFM prevalence: 2018 and 2022. Viral genomes were analyzed to identify major changes between the seasons, and the genomic changes linked to increased hospital admissions were identified.

METHODS

Study Population

Nasopharyngeal swab samples positive for rhinovirus/enterovirus (RV/EV), following the standard-of-care diagnosis at the Johns Hopkins Health System per the GenMark ePlex respiratory pathogen panels [13], were collected for EV-D68 screening, genotyping, and whole genome sequencing. Samples with more than 1 detectable pathogen with the standard-of-care panel testing were classified as coinfections. All available leftover RV/EV-positive samples with collection dates between January 2018 and December 2022 were collected for EV-D68 screening. Samples were collected from inpatients and outpatients within the state of Maryland. Notably, genomes from our group's 2022 study were included in the analysis [7].

EV-D68 Detection

Viral RNA extraction was performed with the chemagic Viral DNA/RNA 300 Kit. Samples collected from January to December 2018 and 2022 were screened for EV-D68 by real-time reverse transcription polymerase chain reaction as described before [14–16]. EV-D68–positive samples from 2019 and 2020 were characterized by typing as described by Nix et al [17]. Samples characterized by our group in 2021 [5] were also included in our cohort. Supplementary Figure 1 details the numbers of patients and samples used for each part of the study.

EV-D68 Whole Genome Sequencing and Phylogenetic Analysis

Whole genome sequencing was performed as we described previously [7]. Updated primers for whole genome amplification were used (Supplementary Table 1). Amplicons of 4363 and 3195 base pairs from the first and second fragment amplification, respectively, were pooled, barcoded with the Native barcoding genomic DNA kit (EXP-NBD196) according to the manufacturer's instructions, and sequenced with R10.4.1 flow cells on a PromethION 2 Solo device (Oxford Nanopore Technologies). The FASTQ files were analyzed by an in-house pipeline. A database comprising all RV/EV reference genomes, including the Fermon EV-D68 strain (AY426531), was used to identify the closest reference. Draft genomes were generated by mini_assemble within pomoxis (version 0.3.15). The draft genome was refined and a consensus sequence established by medaka consensus (version 2.0.1). The quality of genomes, including evaluation of the depth of sequencing, was conducted with samtools depths (version 1.21).

Identification of the EV-D68 clade and subclade was carried out with the RIVM genotyping tool (http://www.rivm.nl/mpf/enterovirus/typingtool/) by complete and partial genome sequences obtained after sequencing. Alignment of the complete genome sequences used for the phylogenetic analysis was performed with Mafft (version 7.450). Maximum likelihood trees for the complete genomes and 5′ UTR sequences were constructed via IQ-TREE2 (version 2.0.6), with 1000 bootstrap replicates. The ModelFinder, implemented in IQ-TREE2, was used to select the best-fitted nucleotide substitution model. The Fermon strain was used to root the trees. The trees were visualized with FigTree version 1.4.4. The amino acid (AA) sequence alignment was performed by MEGA software version 7.0.26. To identify and quantify AA substitutions, sequences of subclade B3 from 2018 and 2022 were compared with the Fermon reference with an in-house script via Python (version 3.11.4). Briefly, the pipeline was developed with the Biopython library to detect AA changes. This pipeline compares sequences with a reference sequence, identifying mutations and compiling the results into a CSV file that includes the position, substituted AA, number of sequences with the mutation, total sequences analyzed, frequency percentage, and the corresponding viral encoded protein.

Clinical Data

Data on patient demographics, comorbidities, positive laboratory results, and clinical course were bulk extracted from the common electronic medical record system by an experienced data analyst (E. K.).

Statistical Analysis

To evaluate the relationship between EV-D68 mutations and AA substitutions and clinical outcomes, we first performed a latent class analysis to assess mutational clusters across the protein coding regions and 5′ UTR segments. Analysis evaluated both sections separately as well as combined for the mutation/substitution and the absence of the mutation/substitution (eg, when D554E was D and when it was E). Univariate logistic analysis was then done on individual mutations and across most likely clusters on the dependent variable of RV/EV-related hospitalization, which were patients admitted with RV/EV infection and no other positive viral test results (eg, excludes patients who may have been coinfected). Significant univariate results were tested in a multivariate logistic analysis that included patient demographics (age, sex, race/ethnicity) and comorbidities and were retained if they remained significant. Odds ratios (ORs) were adjusted for all variables through multivariate models.

Patient Consent Statement and Data Availability

The research was conducted with a waiver of consent under Johns Hopkins Institutional Review Board protocol IRB00221396. Genomes were made publicly available in GenBank: PQ238557-PQ238727, OP572035-OP572095, and OP321139-OP321153.

RESULTS

Characteristics of Patients Infected With EV-D68

In 2018, a total of 10 734 samples were tested with the extended respiratory panel, of which 1701 (15.8%) were positive for RV/EV (Supplementary Table 2). In 2022, a total of 11 948 samples were tested, and 1501 (12.6%) were RV/EV positive. A total of 1807 RV/EV-positive samples were screened for EV-D68 between January and December 2018 (52.9%, 956/1807) and January and December 2022 (47.1%, 851/1807). Among these, 18% (326/1807) tested positive for EV-D68: 11.9% (114/956) in 2018 and 24.9% (212/851) in 2022. Previously identified EV-D68 from 2019 (1), 2020 (6), and 2021 (18) were included in our study cohort, totaling 351 EV-D68 cases (Supplementary Tables 3 and 4).

Demographic and clinical data are detailed in Supplementary Tables 3 to 6. Clinical data were missing for 12 patients from 2018 (Supplementary Figure 1). Of the 339 patients infected with EV-D68 who had complete clinical data, ages ranged from 10 days to 85 years, with a median of 5 years. The majority of cases (50.7%) were in children aged <5 years, followed by those in the group aged 6 to 17 years (21.2%). In terms of race and ethnicity, the highest number of cases were in Black individuals (47.4%), followed by White individuals (26.5%) and then Hispanic (12.6%). The most common comorbidity was asthma (45.7%), followed by cancer (30.9%) and immunosuppression (32.4%). More than half of the cases (55.5%) were admitted to the hospital, with 50% of the admissions being EV infection related. Among all patients with clinical data, 46.9% required supplemental oxygen, and 22.4% needed intensive care unit (ICU)–level care (Supplementary Table 3).

To further understand the association between EV-D68 and EV-related hospitalization, the need for supplemental oxygen, and ICU-level care, we conducted a multivariable regression analysis. Hispanic patients were more likely to be admitted (OR, 2.27; 95% CI, 1.03–5.03) and to require supplemental oxygen (OR, 3.47; 95% CI, 1.53–7.86). Patients with asthma were at higher risk of hospitalization (OR, 2.47; 95% CI, 1.4–4.33), requiring supplemental oxygen (OR, 5.57; 95% CI, 3.15–9.85), and ICU-level care (OR, 2.29; 95% CI, 1.15–4.55; Table 1). Interestingly, patients diagnosed in 2018 showed the highest odds of hospitalization (OR, 6.60; 95% CI, 3.32–13.12), supplemental oxygen (OR, 2.72; 95% CI, 1.43–5.21), and ICU-level care (OR, 4.41; 95% CI, 2.18–8.91).

Genomic Characterization of EV-D68

Of the total 351 samples positive for EV-D68 according to polymerase chain reaction, 272 were successfully genotyped: 34.2% (93/272) were collected in 2018, 0.4% (1/272) in 2019, 1.1% (3/272) in 2020, 6.3% (17/272) in 2021, and the majority (58.1%, 158/272) in 2022. Two subclades, B3 (95.2%, 259/272) and A2/D1 (4.8%, 13/272), were identified. In 2018, B3 and A2/D1 cocirculated with B3 predominating (85/93). In 2019 and 2020, only A2/D1 was detected. In 2021, only B3 was detected, and in 2022, B3 circulated predominantly (157/158) with only 1 A2/D1 genome (Figure 1A). Interestingly, A2/D1 was mainly detected in adult patients, with an average age of 51.6 years and a median age of 55 years.

The phylogenetic analysis, performed with 257 complete genomes (86 in 2018, 4 in 2020, 9 in 2021, and 158 in 2022), revealed 3 distinct clusters of EV-D68 subclade B3. The first cluster exclusively encompassed genomes from 2018. The second comprised genomes from 2021 and 6 from 2022. The third cluster was exclusively composed of 2022 genomes. The sporadic 2022 A2/D1 genome was closer to the 2020 strains than to those from 2018.

The phylogenetic tree generated from the 5′ UTR sequences, consistent with the tree obtained from the complete genome sequences, showed distinct clustering of the 2018 and 2022 genomes. However, some diversity was observed within the 2022 genomes (Figure 1B). The alignment of the 5′ UTR sequences from positions 45 to 732 with the reference genome revealed 5 main differences between the 2018 and 2022 sequences: U109C, U158C, U335C, G714C, and A730C. Notably, 2 mutations were located in domain II: U109C in 39% of the 2022 sequences as opposed to 2% in 2018 and U158C in 94% of the 2018 sequences but in only 10% of the 2022 genomes. U335C (located in domain IV) and G714C were predominantly found in the 2022 genomes, with frequencies of 89% vs 6% and 99% vs 13%, respectively. Substitution A730C was exclusively identified in the 2022 genomes.

A comparative analysis of EV-D68 subclade B3 whole genomes from 2018 and 2022 was performed (228 complete genomes). To identify AA substitutions within our sequences, we conducted an alignment between the coding region of the 2018 and 2022 sequences, alongside the Fermon reference sequence. We identified 80 and 85 changes (identified in at least 10% of all genomes) in 2018 and 2022, respectively, as compared with the reference strain. The majority of these changes were in the capsid proteins (VP1, VP2, and VP3) and in the polymerase (3D; Figure 2). Differences between the 2018 and 2022 genomes were observed at 10 positions: 18, 364, 554, 650, 876, 918, 945, 1445, 1943, and 2183. Some of these substitutions were at antigenic sites within VP1 (BC_Loop), creating a diversity in antigenic sites. The epitope pattern DHTSSTAQ**T**DKNFF was mainly detected in 2018 and 2022, with rates of 89.6% and 57.1%. Another epitope pattern, DHTSSTAQ**A**DKNFF, was exclusively observed in 2022, with a frequency of 39.1% (Supplementary Figure 2A). These 2 main BC loop epitope patterns differed due to an AA substitution at position 98 of the VP1 protein, where the T in the predominant motif and that of the Fermon strain were replaced by an A. Other patterns were detected in both years but identified in <10% of genomes for each year. The DE loop showed less diversity across the years

Table 1. Multivariate Regression Results of the Association Between EV-D68 and EV-Related Hospitalization, Supplemental Oxygen, and ICU Level of Care

	Odds Ratio (95% CI)		
	EV-Related Hospitalization	Supplemental Oxygen	ICU Level of Care
Female	1.19 (.70–2.02)	0.75 (.45–1.26)	1.00 (.55–1.83)
Patient age, y			
0–5	1 [Reference]	1 [Reference]	1 [Reference]
6–17	0.84 (.43–1.67)	1.45 (.73–2.86)	1.20 (.58–2.48)
18–44	0.74 (.26–2.09)	0.45 (.16–1.24)	0.11 (.02–.53)
45–64	1.02 (.20–5.10)	1.40 (.35–5.58)	0.04 (.00–.47)
≥65	1.20 (.20–7.31)	0.74 (.17–3.24)	0.08 (.01–.71)
Race and ethnicity			
Black	1 [Reference]	1 [Reference]	1 [Reference]
Hispanic	**2.27 (1.03–5.03)**	3.47 (1.53–7.86)	1.09 (.42–2.81)
Other	1.40 (.62–3.20)	1.36 (.60–3.08)	0.83 (.30–2.29)
White	1.97 (.97–4.01)	1.62 (.82–3.18)	1.26 (.58–2.74)
Comorbidities			
Asthma	**2.47 (1.40–4.33)**	**5.57 (3.15–9.85)**	**2.29 (1.15–4.55)**
Atrial fibrillation	0.51 (.08–3.35)	1.72 (.36–8.29)	0.41 (.03–5.38)
Cancer	0.78 (.36–1.69)	0.61 (.29–1.26)	0.37 (.16–.89)
Cerebrovascular disease	1.13 (.36–3.53)	0.72 (.23–2.23)	1.06 (.28–4.10)
Coronary artery disease	**3.64 (1.05–12.59)**	0.47 (.14–1.56)	2.12 (.47–9.55)
Diabetes	0.99 (.32–3.12)	0.40 (.14–1.12)	1.07 (.29–3.99)
Heart failure	1.30 (.32–5.32)	1.35 (.40–4.60)	0.85 (.22–3.33)
Hypertension	1.69 (.73–3.90)	1.62 (.74–3.54)	1.49 (.61–3.64)
Immunosuppression	**2.19 (1.01–4.77)**	1.45 (.70–3.03)	1.63 (.70–3.76)
Kidney disease	0.61 (.22–1.68)	0.89 (.35–2.28)	0.71 (.23–2.24)
Lung disease	0.67 (.16–2.73)	**3.51 (1.05–11.72)**	4.04 (.76–21.55)
Smoker	2.02 (.49–8.35)	1.65 (.52–5.18)	1.68 (.40–7.08)
Emergency department visit	2.82 (1.44–5.52)	1.86 (.98–3.51)	0.50 (.24–1.02)
2018	**6.60 (3.32–13.12)**	**2.72 (1.43–5.21)**	**4.41 (2.18–8.91)**
2019–2021	0.65 (.21–2.00)	1.68 (.60–4.71)	1.66 (.51–5.41)
2022	1 [Reference]	1 [Reference]	1 [Reference]

Bold indicates $P < .05$.

Abbreviations: EV, enterovirus; EV-D68, enterovirus D68; ICU, intensive care unit.

(Supplementary Figure 2B). The predominant epitope sequence NGSNNNTYV had a frequency of 89% in all years, while all other epitope patterns were at <6%. In addition to the substitutions detected in the VP1 epitopes, some changes—including T918A (2A: T57A), N945S (2A: N84S), I1445V (3A: I9V), and I1943M (3D: I212M)—were exclusively detected in 2022, with frequencies of 42%, 100%, 93%, and 92%. AA changes I364V and N554D, which were present in >95% of the 2018 genomes, decreased in frequency to about 7% in 2022. We also observed an increase in the frequency of N554E (96%), T650A (40%), and K2183R (77%) in 2022, while their frequencies did not exceed 10% in 2018.

Latent class analysis found a single dominant cluster (concomitant changes) in the 5′ UTR group and 1 in the polyprotein coding group but no dominant clusters across both groups (Supplementary Tables 5 and 6 detail the metadata of patients used for this analysis). Univariate analysis with individual mutations, AA substitutions, and each cluster found that only the clusters were significant. The 2018 cluster of AA—554D, 650T, 918T, 945N, 1445I, and 1943I—was significant in the multivariate analysis (Table 2) and was significantly associated with RV/EV-related admission (OR, 12.47; 95% CI, 4.51–34.49) and the need for supplemental oxygen (OR, 3.18; 95% CI, 1.40–7.23). The only other factor associated with either outcome was asthma.

DISCUSSION

EV-D68 infections exhibit a distinct seasonal pattern, typically peaking in late summer and early fall. Significant outbreaks of EV-D68 have occurred in 2014, 2016, 2018, and 2022, primarily affecting children and displaying a potential biennial circulation. Coinciding with all but the 2022 outbreak, AFM cases have also shown seasonal peaks in late summer and early fall [1]. The temporal and geographic correlation between EV-D68 outbreaks and spikes in AFM cases suggests a potential link, though establishing a definitive causal relationship remains challenging due to diagnostic difficulties and infrequent

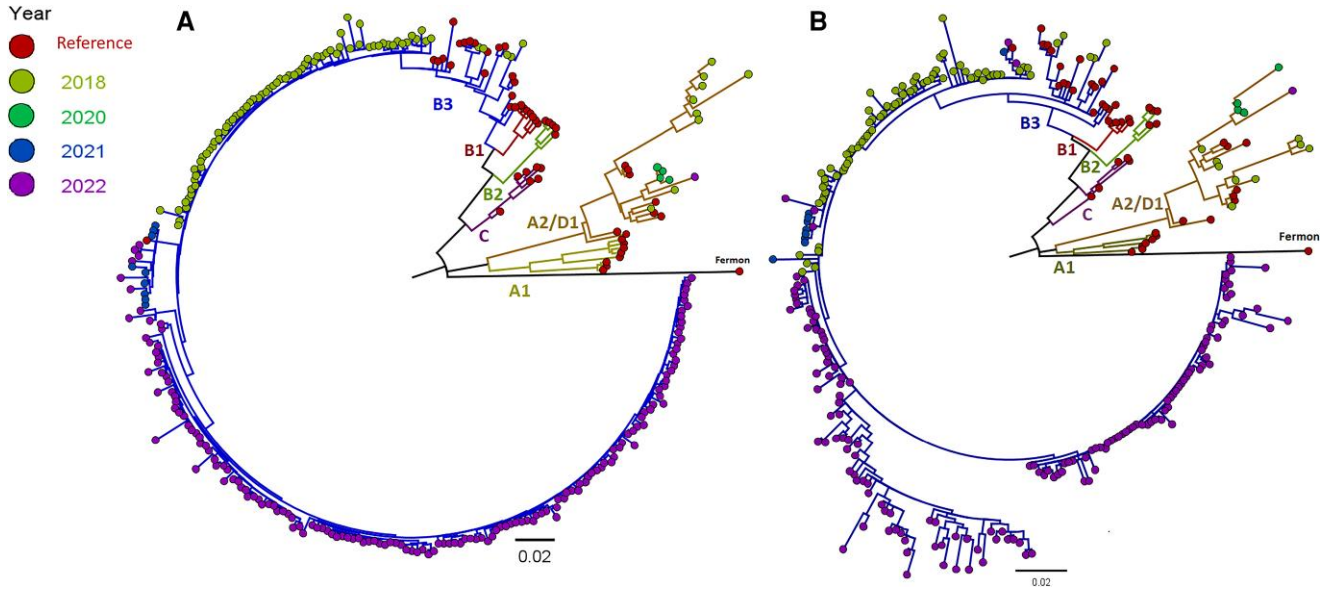

Figure 1. *A*, Phylogenetic relationships of EV-D68 genomes identified from the Johns Hopkins Health System from January 2018 to December 2022. *B*, Phylogenetic tree of the 5′ UTR of EV-D68 genomes. The phylogenetic trees were constructed via the maximum likelihood method in IQ-TREE2 with 1000 bootstrap replicates and is rooted by the Fermon strain. EV-D68, enterovirus D68.

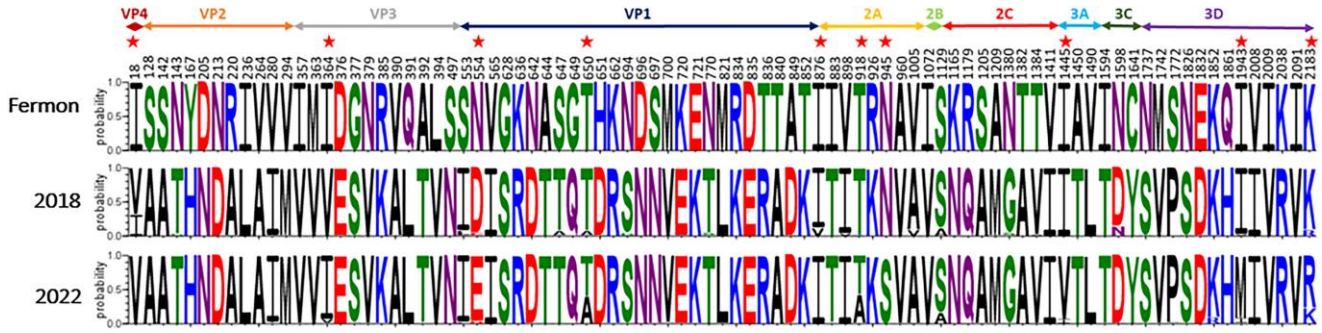

Figure 2. Amino acid polymorphisms with frequencies ≥10% in our 2018 and 2022 B3 subclade complete genomes as compared with the Fermon reference strain. Asterisks indicate the differences observed between the 2018 and 2022 genomes at positions 18, 364, 554, 650, 876, 918, 945, 1445, 1943, and 2183.

viral detection in CSF. Understanding the circulation and genomic evolution of EV-D68 is crucial for elucidating the virus's pathogenicity, even if the studied cohort does not include AFM cases.

In this retrospective study, we analyzed the outcomes of EV-D68 infections and their genomic evolution from 2018 to 2022. We focused on comparing the 2 outbreak years, 2018 and 2022, which had different prevalence rates of AFM. A comparative analysis of outcomes collected from both years showed that the EV-D68 outbreak in 2018 appeared to be more severe than that of 2022, with higher probabilities of requiring supplemental oxygen, admissions, and ICU care. Although cases of AFM were not reported in our study, the 2018 EV-D68 outbreak coincided with cases of AFM, whereas very few cases were noted in 2022 [1]. Detailed genomic/outcome analyses revealed that the 2018 AA cluster 554D, 650T, 918T, 945N, 1445I, and 1943I was significantly associated with increased EV-D68 admissions and requiring supplemental oxygen.

Phylogenetic analysis of our sequences from 2018 and 2022 revealed the predominant circulation of the EV-D68 subclade B3 in both years, with a few cases of subclade A2/D1 detected in 2018. However, subclade B3 primarily formed 2 clusters, each specific to a particular year. Alignment of the polyprotein sequences with the Fermon strain identified 10 AA substitutions between the 2018 and 2022 genomes (at positions 18, 364, 554, 650, 876, 918, 945, 1445, 1943, and 2183). Substitutions occurred in VP1, resulting in various antigenic epitope patterns. The pattern DHTSSTAQ**T**DKNFF was

Table 2. Odds Ratios of Outcomes in Patients Infected With EV-D68 in 2018 and 2022 and With a Characterized Complete Genome Sequence

	Odds Ratio (95% CI)	
	EV-Related Hospitalization	Supplemental Oxygen
Female	0.88 (.44–1.78)	0.65 (.32–1.30)
Patient age, y		
0–5	1 [Reference]	1 [Reference]
6–17	1.24 (.45–3.42)	0.60 (.22–1.63)
18–44	0.97 (.36–2.61)	0.74 (.28–1.98)
45–64	0.72 (.15–3.43)	0.30 (.07–1.35)
≥65	1.76 (.11–29.24)	0.24 (.02–2.46)
Race and ethnicity		
Black	1 [Reference]	1 [Reference]
Hispanic	1.70 (.60–4.77)	2.14 (.76–6.02)
Other	1.46 (.52–4.08)	0.67 (.24–1.86)
White	3.91 (1.45–10.54)	1.36 (.55–3.35)
Comorbidities		
Asthma	**2.57 (1.20–5.50)**	**6.69 (3.14–14.24)**
Atrial fibrillation	1.55 (.07–33.23)	8.71 (.59–127.85)
Cancer	0.64 (.22–1.90)	0.83 (.31–2.19)
Cerebrovascular disease	0.75 (.16–3.51)	0.53 (.12–2.43)
Coronary artery disease	4.89 (.74–32.27)	0.38 (.07–2.16)
Diabetes	1.28 (.20–8.08)	0.35 (.06–1.97)
Heart failure	0.51 (.06–3.93)	1.44 (.24–8.51)
Hypertension	1.44 (.51–4.12)	1.26 (.47–3.37)
Immunosuppression	2.47 (.91–6.73)	1.88 (.73–4.85)
Kidney disease	0.74 (.19–2.91)	0.52 (.15–1.79)
Lung disease	1.18 (.14–10.05)	3.85 (.72–20.53)
Emergency department visit	2.40 (1.00–5.81)	1.71 (.75–3.87)
Amino acid substitution cluster[a]	**12.47 (4.51–34.49)**	**3.18 (1.40–7.23)**

Bold indicates $P < .05$.

Abbreviations: EV, enterovirus; EV-D68, enterovirus D68.

[a]Defined as the 2018 amino acid cluster: 554D, 650T, 918T, 945N, 1445I, 1943I.

prevalent in both years, while DHTSSTAQA**D**KNFF was observed in only 2022. The latter was significantly associated with higher viral loads in respiratory samples and requiring supplemental oxygen in a previous study by our group [7]. While higher viral load can indicate increased viral replication, it may not necessarily correlate with severe clinical disease. T650A (VP1: T98A), which distinguishes these epitopes, is located in a loop region surrounding the "canyon" area responsible for host-receptor interaction and is expected to alter the polarity of the side chain [18]. The BC loop pattern of the US 2018 B3 subclade does not appear to have been previously observed in the United States [19]. This may have contributed to the higher severity observed during that year's outbreak vs 2022. Indeed, the BC and DE loops are the most variable regions of the VP1 protein and contain immunogenic neutralizing antibody binding sites. Such variability could contribute to the severity of an outbreak by evading immune responses [20, 21]. Notably, a previous report by our group cited atypical neurologic presentation associated with enterovirus infection in a patient with hypogammaglobulinemia, further supporting the role of antibodies in protecting against enterovirus-mediated neurologic disease [22].

In addition to the AA changes detected in the antigenic epitopes, some substitutions, including 2A:T57A, 2A:N84S, 3A:I9V, and 3D:I212M, were exclusively detected in 2022. Notably, N84T is near the active site of the 2A protease and is known to confer resistance to the drug telaprevir but reduces the viral replication efficiency [23]. AA substitution T57A (2A) is in close proximity to G58, which has been identified as a critical contact residue involved in the interaction with the host cell protein SETD3 [24].

The comparison between our 2018 and 2022 5′ UTR sequences revealed 5 major differences, including the U109C and U158C located in domain II. Interestingly, it has been reported that a single nucleotide change from cytosine to uridine at base 158 in the 5′ UTR reduced viral translation and virulence of EV71 in mice [25].

Our study identified a cluster of AA that was significantly associated with severe outcomes. Dissecting the clinical significance of each AA substitution in our cohort is not possible due to the co-occurrence of these changes. Therefore, it is important to supplement clinical and genomic surveillance studies with in vitro models that can identify the significance of each mutation to neurovirulence or viral fitness.

A recent study using chimeric viruses of two 2014 EV-D68 strains demonstrated that VP1 could be the main determinant of EV-D68 neurovirulence. The strain causing paralysis differed by 4 VP1 substitutions: S553L, D554N, A650T, and K835E [26]. Interestingly, our study highlighted the significant association of the 2018 genotypes of AA sites 554 (D) and 650 (T) with severe clinical outcomes. Follow-up in vitro studies and upcoming season's genomic viral surveillance should reveal the contribution of these changes to viral pathogenesis.

Enteroviruses are classified by the homology of the P1 region or the *VP1* gene into multiple species that comprise >100 types [17, 27]. More than 40 EV genotypes have been identified in AFM cases. So far, the causal relationship between EV-D68 and AFM has not been established. Limitations in identifying the virus in CSF at the time of AFM presentation might largely be due to the delay between the respiratory disease and neurologic presentation and challenges in sample collections [28]. That said, studies showed that in patients with AFM, EV-D68 antibodies are readily detectable when compared with control patients [29, 30]. While viral evolution can reportedly modulate enterovirus neurovirulence [31–34], factors such as preexisting immune response and genetic susceptibility may contribute to an AFM outcome. Our study is limited by the potential sample collection bias. Clinical testing for enterovirus is usually performed for pediatric, immunocompromised, or hospitalized cases. This may limit the generalizability of our findings to a broader community setting. In addition, the retrospective nature of the study restricts access to data that include prior

infections or vaccinations. The strict criteria used for defining enterovirus-associated admissions do not exclude the likelihood of the contribution of other underlying conditions to the decision of admitting patients in our cohort.

Supplementary Data

Supplementary materials are available at *Open Forum Infectious Diseases* online. Consisting of data provided by the authors to benefit the reader, the posted materials are not copyedited and are the sole responsibility of the authors, so questions or comments should be addressed to the corresponding author.

Notes

Financial support. This work was supported by the Johns Hopkins Department of Pathology.

Potential conflicts of interest. H. H. M. collaborates for research with Hologic and Diasorin. H. H. M. received honoraria from Roche Diagnostics and BD Diagnostics and serves on the advisory board of Seegene. All other authors report no potential conflicts.

References

1. Whitehouse ER, Lopez A, English R, et al. Surveillance for acute flaccid myelitis—United States, 2018–2022. MMWR Morb Mortal Wkly Rep **2024**; 73:70–6.
2. Andres C, Vila J, Creus-Costa A, et al. Enterovirus D68 in hospitalized children, Barcelona, Spain, 2014–2021. Emerg Infect Dis **2022**; 28:1327–31.
3. Benschop KS, Albert J, Anton A, et al. Re-emergence of enterovirus D68 in Europe after easing the COVID-19 lockdown, September 2021. Euro Surveill **2021**; 26:2100998.
4. Erster O, Bar-Or I, Levy V, et al. Monitoring of enterovirus D68 outbreak in Israel by a parallel clinical and wastewater based surveillance. Viruses **2022**; 14:1010.
5. Fall A, Gallagher N, Morris CP, et al. Circulation of enterovirus D68 during period of increased influenza-like illness, Maryland, USA, 2021. Emerg Infect Dis **2022**; 28:1525–7.
6. Shah MM, Perez A, Lively JY, et al. Enterovirus D68-associated acute respiratory illness horizontal line new vaccine surveillance network, United States, July–November 2018–2020. MMWR Morb Mortal Wkly Rep **2021**; 70:1623–8.
7. Fall A, Han L, Abdullah O, et al. An increase in enterovirus D68 circulation and viral evolution during a period of increased influenza like illness, The Johns Hopkins Health System, USA, 2022. J Clin Virol **2023**; 160:105379.
8. Ma KC, Winn A, Moline HL, et al. Increase in acute respiratory illnesses among children and adolescents associated with rhinoviruses and enteroviruses, including enterovirus D68—United States, July–September 2022. MMWR Morb Mortal Wkly Rep **2022**; 71:1265–70.
9. Simoes MP, Hodcroft EB, Simmonds P, et al. Epidemiological and clinical insights into the enterovirus D68 upsurge in Europe 2021/22 and the emergence of novel B3-derived lineages, ENPEN multicentre study. J Infect Dis **2024**; 230:e917–28
10. Helfferich J, Neuteboom RF, de Lange MMA, et al. Pediatric acute flaccid myelitis: evaluation of diagnostic criteria and differentiation from other causes of acute flaccid paralysis. Eur J Paediatr Neurol **2023**; 44:28–36.
11. Messacar K, Spence-Davizon E, Osborne C, et al. Clinical characteristics of enterovirus A71 neurological disease during an outbreak in children in Colorado, USA, in 2018: an observational cohort study. Lancet Infect Dis **2020**; 20:230–9.
12. Messacar K, Asturias EJ, Hixon AM, et al. Enterovirus D68 and acute flaccid myelitis—evaluating the evidence for causality. Lancet Infect Dis **2018**; 18:e239–47.
13. Jarrett J, Uhteg K, Forman MS, et al. Clinical performance of the GenMark Dx ePlex respiratory pathogen panels for upper and lower respiratory tract infections. J Clin Virol **2021**; 135:104737.
14. Fall A, Ndiaye N, Messacar K, et al. Enterovirus D68 subclade B3 in children with acute flaccid paralysis in West Africa, 2016. Emerg Infect Dis **2020**; 26:2227–30.
15. Fall A, Ndiaye N, Jallow MM, et al. Enterovirus D68 subclade B3 circulation in Senegal, 2016: detection from influenza-like illness and acute flaccid paralysis surveillance. Sci Rep **2019**; 9:13881.
16. Fall A, Jallow MM, Kebe O, et al. Low circulation of subclade A1 enterovirus D68 strains in Senegal during 2014 North America outbreak. Emerg Infect Dis **2019**; 25:1404–7.
17. Nix WA, Oberste MS, Pallansch MA. Sensitive, seminested PCR amplification of VP1 sequences for direct identification of all enterovirus serotypes from original clinical specimens. J Clin Microbiol **2006**; 44:2698–704.
18. Du J, Zheng B, Zheng W, et al. Analysis of enterovirus 68 strains from the 2014 North American outbreak reveals a new clade, indicating viral evolution. PLoS One **2015**; 10:e0144208.
19. Hodcroft EB, Dyrdak R, Andres C, et al. Evolution, geographic spreading, and demographic distribution of enterovirus D68. PLoS Pathog **2022**; 18:e1010515.
20. Pabbaraju K, Wong S, Drews SJ, Tipples G, Tellier R. Full genome analysis of enterovirus D-68 strains circulating in Alberta, Canada. J Med Virol **2016**; 88: 1194–203.
21. Liu Y, Sheng J, Fokine A, et al. Structure and inhibition of EV-D68, a virus that causes respiratory illness in children. Science **2015**; 347:71–4.
22. Fall A, Forman M, Morris CP, et al. Enterovirus characterized from cerebrospinal fluid in a cohort from the Eastern United States. J Clin Virol **2023**; 161:105401.
23. Musharrafieh R, Ma C, Zhang J, et al. Validating enterovirus D68–2A(pro) as an antiviral drug target and the discovery of telaprevir as a potent D68-2A(pro) inhibitor. J Virol **2019**; 93:e02221-18.
24. Peters CE, Schulze-Gahmen U, Eckhardt M, et al. Structure-function analysis of enterovirus protease 2A in complex with its essential host factor SETD3. Nat Commun **2022**; 13:5282.
25. Yeh MT, Wang SW, Yu CK, et al. A single nucleotide in stem loop II of 5′-untranslated region contributes to virulence of enterovirus 71 in mice. PLoS One **2011**; 6:e27082.
26. Leser JS, Frost JL, Wilson CJ, Rudy MJ, Clarke P, Tyler KL. VP1 is the primary determinant of neuropathogenesis in a mouse model of enterovirus D68 acute flaccid myelitis. J Virol **2024**; 98:e0039724.
27. Knipe DM, Howley PM. Enteroviruses: polioviruses, coxsackieviruses, echoviruses, and newer enteroviruses. 4th ed. Philadelphia, PA: Lippincott Williams & Wilkins, **2001**.
28. Grizer CS, Messacar K, Mattapallil JJ. Enterovirus-D68—a reemerging non-polio enterovirus that causes severe respiratory and neurological disease in children. Front Virol **2024**; 4:1328457.
29. Mishra N, Ng TFF, Marine RL, et al. Antibodies to enteroviruses in cerebrospinal fluid of patients with acute flaccid myelitis. mBio **2019**; 10:e01903-19.
30. Schubert RD, Hawes IA, Ramachandran PS, et al. Pan-viral serology implicates enteroviruses in acute flaccid myelitis. Nat Med **2019**; 25:1748–52.
31. Pallansch MA, Oberste MS, Whitton JL. Enteroviruses: polioviruses, coxsackieviruses, echoviruses, and newer enteroviruses. In: Knipe DM, Howley PM. Fields virology. Philadelphia, PA: Lippincott Williams & Wilkins, **2013**:490–530.
32. Combelas N, Holmblat B, Joffret ML, Colbere-Garapin F, Delpeyroux F. Recombination between poliovirus and coxsackie A viruses of species C: a model of viral genetic plasticity and emergence. Viruses **2011**; 3:1460–84.
33. Link-Gelles R, Lutterloh E, Schnabel Ruppert P, et al. Public health response to a case of paralytic poliomyelitis in an unvaccinated person and detection of poliovirus in wastewater—New York, June–August 2022. MMWR Morb Mortal Wkly Rep **2022**; 71:1065–8.
34. Russo GB, Goyal T, Tyler K, Thakur KT. Re-emergence of poliovirus in the United States: considerations and implications. Ann Neurol **2022**; 92:725–8.